Heliyon 9 (2023) e23242

Contents lists available at ScienceDirect

Heliyon

journal homepage: www.cell.com/heliyon

A radiomics approach based on MR imaging for classification of deficiency and excess syndrome of traditional Chinese medicine in prostate cancer

Yongsheng Zhang [a,1], Huan Yang [b,1], Zhiping Li [a], Chen Gao [c], Yin Chen [d], Yasheng Huang [d], Xianjie Yue [a], Chang Shu [e], Yuguo Wei [f], Feng Cui [a], Maosheng Xu [c,*]

[a] Department of Radiology, Hangzhou TCM Hospital Affiliated to Zhejiang Chinese Medical University, Hangzhou, 310007, China
[b] Department of Acupuncture and Moxibustion, Community Health Service of Xiaohehushu District, Hangzhou, 310005, China
[c] Department of Radiology, The First Affiliated Hospital of Zhejiang Chinese Medical University (Zhejiang Provincial Hospital of Chinese Medicine), Hangzhou, 310006, China
[d] Department of Urology, Hangzhou TCM Hospital Affiliated to Zhejiang Chinese Medical University, Hangzhou, 310007, China
[e] Department of Pathology, Hangzhou TCM Hospital Affiliated to Zhejiang Chinese Medical University, Hangzhou, 310007, China
[f] Advanced Analytics, Global Medical Service, GE Healthcare, Hangzhou, 310007, China

ARTICLE INFO

Keywords:
Prostate cancer
TCM syndrome
Magnetic resonance imaging
Radiomic

ABSTRACT

Objective: To explore the potential imaging biomarkers for predicting Traditional Chinese medicine (TCM) deficiency and excess syndrome in prostate cancer (PCa) patients by radiomics approach based on MR imaging.

Methods: A total of 121 PCa patients from 2 centers were divided into 1 training cohort with 84 PCa patients and 1 validation cohort with 37 PCa patients. The PCa patients were divided into deficiency and excess syndrome group according to TCM syndrome differentiation. Radiomic features were extracted from T2-weighted imaging (T2WI), diffusion-weighted imaging and apparent diffusion coefficient images originated from diffusion-weighted imaging. A radiomic signature was constructed after reduction of dimension in training group by the minimum redundancy maximum relevance and the least absolute shrinkage and selection operator. The performance of the model was evaluated by receiver operating characteristic (ROC) curve and calibration curve.

Results: The radiomic scores of PCa with TCM excess syndrome group were statistically higher than those of PCa with TCM deficiency syndrome group among T2WI, diffusion-weighted imaging and apparent diffusion coefficient imaging models. The area under ROC curves for T2WI, diffusion-weighted imaging and apparent diffusion coefficient imaging models were 0.824, 0.824, 0.847 in the training cohort and 0.759, 0.750, 0.809 in the validation cohort, respectively. The apparent diffusion coefficient imaging model had the best discrimination in separating patients with TCM excess syndrome and deficiency syndrome, and its accuracy was 0.788, 0.778 in the training and validation cohort, respectively. The calibration curve demonstrated that there was a high consistency between the prediction of radiomic scores and the actual classification of TCM's deficiency and excess syndrome in PCa.

* Corresponding authors.
E-mail addresses: feng6812@163.com (F. Cui), xums166@zcmu.edu.cn (M. Xu).
[1] Yongsheng Zhang and Huan Yang contributed equally to this work.

https://doi.org/10.1016/j.heliyon.2023.e23242
Received 20 May 2023; Received in revised form 28 November 2023; Accepted 29 November 2023
Available online 3 December 2023

Conclusion: The radiomic signature based on MR imaging can be performed as a non-invasive, potential approach to discriminate TCM deficiency syndrome from excess syndrome in PCa, in which apparent diffusion coefficient imaging model has the best diagnostic efficiency.

1. Introduction

Prostate cancer (PCa) is the second most common malignancy in men worldwide [1]. The incidence of PCa in China is lower than that in Western countries, but both the morbidity and mortality have shown a significant increase in recent years [2]. Traditional Chinese medicine (TCM) has played an important role in the treatment of PCa , particularly for advanced patients. TCM syndrome is the pathological generalization of pathogenesis, the degree of severity and development trend of diseases at specific stages [3,4]. Each TCM physician classified and treated PCa based on their respective experience, so there were considerable TCM syndrome patterns [5,6]. Si et al. analyzed 76 literatures on the diagnosis and treatment of PCa by related TCM between 1979 and 2014 and found 31 PCa TCM syndromes and up to 254 individual TCM syndromes [5]. The standard TCM syndrome differentiation of PCa has not yet to be established, which has hindered the development of TCM to some extent. It is necessary to absorb the advantages and methods of modern medicine and artificial intelligence, and mix the objective quantitative indicators into TCM syndrome differentiation and treatment in PCa [7].

Magnetic resonance imaging (MRI) has been currently recognized as the preferred imaging method for prostate-related disease due to its high soft tissue resolution, spatial resolution, functional and morphological definition. MRI plays a dramatic role in PCa detection, localization, targeted biopsy, staging, risk stratification management, and active surveillance [8]. T2-weighted imaging (T2WI), diffusion-weighted imaging (DWI), and its derivative apparent diffusion coefficient (ADC) maps have a leading role in PCa diagnosis and evaluation [9,10].

Radiomics is a powerful approach that can be performed to extract many quantitative features from imaging data and convert the information into mineable data [11]. Recently, studies have hinted at the possibility of diagnosing PCa using MRI-based radiomics [12,13]. Min et al. showed that the area under the curve of multi-parametric MRI-based radiomics for the diagnosis of PCa with Gleason score $\geq 3+4$ was 0.872, 0.823, respectively in the training and test sets [12]. However, the performance of radiomics for predicting PCa's TCM syndrome remains unknown. The two principles of yin and yang, deficiency and excess in the syndrome differentiation of the eight principles of TCM can cover almost all syndromes [14,15]. Based on the theory, it is accessible to conduct the relative research on TCM syndromes that classify and simplify considerable TCM syndromes patterns into two syndromes: deficiency and excess in PCa. Thus, the purpose of the study was to evaluate the value of MRI-based radiomic signatures in differentiating TCM excess and deficiency syndromes in PCa.

2. Materials and methods

2.1. Patient population

This retrospective study was approved by each respective Local Institutional Review Board (No: 2022KY051). It was determined that written informed consent was not needed for a retrospective study. The centers included in this study are Hangzhou TCM Hospital Affiliated to Zhejiang Chinese Medical University (center 1) and The First Affiliated Hospital of Zhejiang Chinese Medical University (center 2). The diagnostic criteria for syndrome differentiation were in accordance with the syndrome classification criteria (TCM Oncology) [15]. The spleen-kidney deficiency syndrome, deficiency syndrome of both qi and yin and Deficiency of Qi and Blood were classified as TCM deficiency syndrome group. The dampness-heat accumulation syndrome, phlegm-blood stasis syndrome and qi stagnation and blood stasis syndrome were classified as TCM excess syndrome group. TCM syndrome differentiation was performed by two associate chief TCM physicians to ensure their uniformity and authority.

Inclusion criteria were as follows: (1) PCa must be confirmed by pathology following radical prostatectomy or prostate biopsy; (2) patients must have obtained MRI imaging on a 3.0 T MRI scanner with T1WI, T2WI and DWI; (3) pathological results must be collected in less than 2 months following MRI examination. The exclusion criteria were as follows: (1) patients with other complications, such as acute respiratory tract infection, urinary tract infection, diabetes, recent cardiovascular disease, etc., interfered with TCM syndrome differentiation; (2) patients had a history of PCa treatment before MRI examination; (3) MRI images were of low quality or the tumor was less than 5 mm in diameter on MRI. Initially, a total of 204 PCa patients were enrolled in the study, and then 83 PCa patients were excluded due to the above exclusion criteria. Finally, 121 PCa patients were enrolled in this study, among which 84 PCa patients from center 1 were performed to be the training cohort, 37 PCa patients from center 2 were selected as the validation cohort to evaluate the model's performance. In the training cohort, there were 45 patients with TCM excess syndrome and 39 patients with TCM deficiency syndrome. There were 15 patients with TCM excess syndrome and 22 patients with TCM deficiency syndrome in the validation cohort. The basic clinical information of patients was obtained from the electronic medical records, including age and prostatic specific antigen (PSA). The interval between MRI and PSA must be within one month.

2.2. MRI acquisition

A 3.0 T MR scanner (GE Discovery MR750 or Siemens Magnetom Verio) was used in all patients, and a pelvic-specific phase-

controlled vibrating coil was applied. Prior to the examination, patients had a moderately filled bladder. The scan range included the entire prostate and seminal vesicle. MRI protocol included axial T1WI, axial and sagittal T2WI, and axial DWI sequences. The b value of DWI was taken as 0–50 s/mm^2, 800–1000 s/mm^2. ADC maps derived from DWI maps were automatically generated by each MR system according to standard mono-exponential models. The detailed scanning sequence and parameters of MR scanners in two hospitals were displayed in Supplementary Table 1.

2.3. Pathological evaluation

The transrectal ultrasound guided 10–12 core systematic biopsy plus cognitive-targeted biopsy were performed. The urologist attempted to specifically target lesions using cognitive registration if MRI-suspected lesions were found. Cores were individually labelled according to their location. The histopathologic reports were assessed with reference to the International Society of Urological Pathology (ISUP) guidelines [16]. An experienced radiologist with 22 years of experience in prostate MRI matched MRI findings and the standard of reference findings and determined index lesion according histopathologic reports, biopsy core location record and radical prostatectomy record.

2.4. Lesion segmentation on MRI

The ITK-SNAP 3.6.0 (www.itk-snap.org) software was performed to delineate the region of interest (ROI). All ROIs were segmented by the radiologist (Z.P.L. with 7 years of experience in prostate MRI) with reference to the pathological results. The tumor was manually segmented to form a three-dimensional ROI volume. For multiple lesion PCa, the index lesion was selected for delineation based on the malignancy and biological behavior of PCa patients determined by the index lesion [17,18]. ROIs were designed to include as much tumor tissue while avoiding surrounding normal tissue. The maximum diameters of the tumors were also measured on T2WI. The MRI T-stage was also assessed on T2WI with reference to NCCN guidelines [19]. The criteria of MRI T-stage were displayed in Supplementary Table 2.

2.5. Radiomic feature extraction

Three-dimensional ROIs from the segmented T2WI, DWI, and ADC images were imported into the Analysis Kit (AK, GE Healthcare, USA) software for the extraction of radiomic features. A total of 1316 radiomic features were extracted from each image, including histogram features, gray level run length matrix (GLRLM), shape, adjacent gray level difference matrix (NGTDM), gray level co-occurrence matrix (GLCM), gray level region size matrix (GLSZM), gray level dependence matrix (GLDM) features and wavelet transforms.

Although the two centers used two different models of MR scanners, the scanning sequences and parameters were different. Therefore, before extracting the imaging features, the T2WI, DWI, and ADC maps of all patients were image resampled (1 * 1 * 1 mm^3) and gray-level normalized (0–255) to reduce the effect of different imaging parameters on the radiomic features. After feature extraction, Z-scores were normalized ((x-μ)/σ, where x is the feature value, μ is the average of all patients in the set for that feature, and σ describes the corresponding standard deviation) for each feature, thereby reducing the impact of the dimension on the feature coefficients and on the machine learning model for classification.

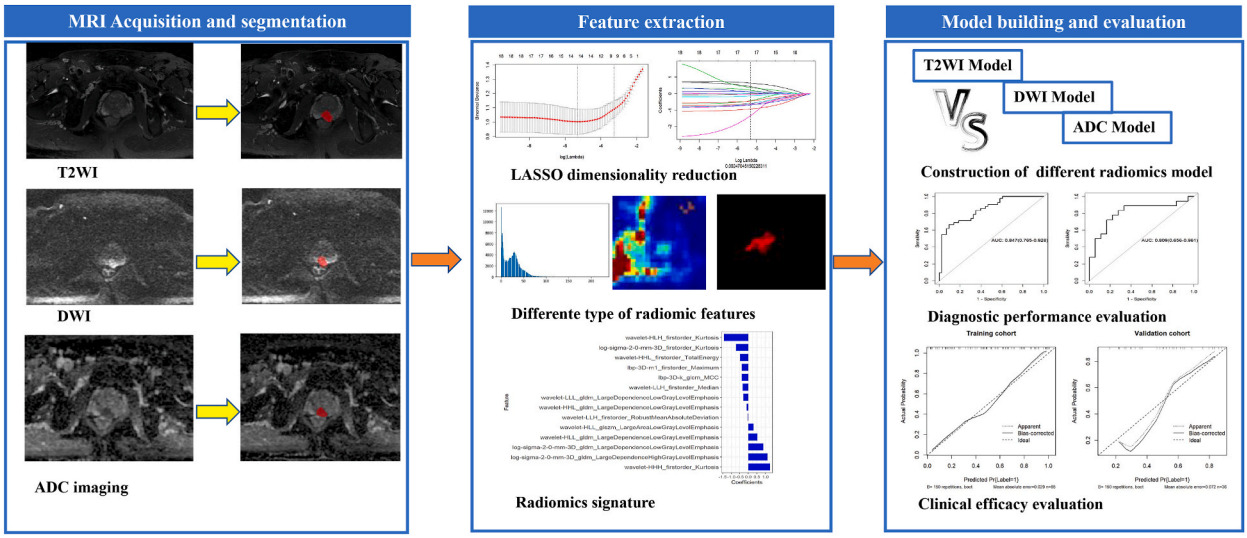

Fig. 1. Workflow of the development of the radiomic model.

2.6. Radiomic signature development

Radiomic signature were developed via two steps: (1) the minimum Redundancy Maximum Relevance (mRMR) was used to eliminate redundant and unrelated features; (2) the least absolute shrinkage and selection operator (LASSO) algorithm was implemented to reduce the coefficients of some features to zero, and key features were selected to construct the final optimized feature set. The optimal λ value was determined by 10-fold cross verification method to achieve the optimal prediction value of radiomic features and calculate their corresponding coefficients. The rad-score was composed of summing the selected features weighted by their coefficients. The details of the radiomics procedure were showed in the Supplementary material II.

The receiver operating characteristic (ROC) curve were adopted to evaluate the discrimination performance in the training and validation cohorts. The calibration curve was used to evaluate the consistency of radiomic signature prediction and the actual classification of TCM's deficiency and excess syndrome in PCa. The fit of the analysis model was tested using the Hosmer Lemeshow test. The Hosmer Lemeshow test is a common method to assess the fit of a logistic regression. When the P value of the test result is greater than 0.05, it indicates that the result classified by logistic regression has a higher fit with the actual occurrence [20]. The radiomics workflow is presented in Fig. 1.

2.7. Statistical analysis

All statistical testing was conducted using R software (version v. 3.5.1) or SPSS 25.0. Continuous variables were analyzed by the independent sample T test or Mann-Whitney *U* test. Categorical variables could also be expressed as the Fishe's exact test or chi-square test when appropriate. The differences in the area under the ROC curve (AUC) of each assessment model were compared with the Delong test. A two-sided *P* value < 0.05 was used to determine statistical significance.

Table 1
Clinical characteristics of patients in the training and validation cohorts.

Characteristics	Training cohort		*P*	Validation cohort		*P*
	deficiency syndrome group (n = 39)	excess syndrome group (n = 45)		deficiency syndrome group (n = 22)	excess syndrome group (n = 15)	
Age (years)	73.56 ± 8.13	73.98 ± 8.93	0.826	72.32 ± 6.25	73.80 ± 7.83	0.527
TPSA (ng/ml)	67.86 ± 173.01	66.55 ± 181.72	0.973	149.88 ± 323.96	84.45 ± 183.04	0.484
fPSA (ng/ml)	5.54 ± 8.09	4.85 ± 8.14	0.696	8.45 ± 13.07	7.16 ± 11.24	0.757
TCM syndrome			NA			NA
	spleen-kidney deficiency syndrome (n = 27)	dampness-heat accumulation syndrome (n = 22)		spleen-kidney deficiency syndrome (n = 13)	dampness-heat accumulation syndrome (n = 7)	
	deficiency syndrome of both qi and yin (n = 7)	phlegm-blood stasis syndrome (n = 13)		deficiency syndrome of both qi and yin (n = 5)	phlegm-blood stasis syndrome (n = 5)	
	Deficiency of Qi and Blood (n = 5)	qi stagnation and blood stasis syndrome (n = 10)		Deficiency of Qi and Blood (n = 4)	qi stagnation and blood stasis syndrome (n = 3)	
Maximum diameter (mm)	20.90 ± 11.28	19.05 ± 10.77	0.446	24.94 ± 17.43	22.86 ± 11.95	0.691
MRI T-stage			0.781			0.386
T2	26 (66.7 %)	33 (73.3 %)		14 (63.64 %)	7 (46.67 %)	
T3	7 (17.9 %)	7 (15.6 %)		5 (22.73 %)	5 (33.33 %)	
T4	6 (15.4 %)	5 (11.1 %)		3 (13.64 %)	3 (20.00 %)	
Location			0.932			0.591
PZ	18 (46.2 %)	19 (42.2 %)		7 (31.82 %)	5 (33.33 %)	
TZ	11 (28.2 %)	14 (31.1 %)		13 (59.09 %)	7 (46.67 %)	
PZ and TZ	10 (25.6 %)	12 (26.7 %)		2 (9.09 %)	3 (20.00 %)	
Lesion number			0.031*	1.41 ± 0.59	1.73 ± 0.88	0.539
1	29 (74.4 %)	36 (80 %)		14 (63.6 %)	7 (46.7 %)	
2	9 (23.1 %)	3 (6.7 %)		7 (31.8 %)	6 (40 %)	
3	1 (2.6 %)	6 (13.3 %)		1 (4.5 %)	2 (13.4 %)	
Gleason score			0.535			0.127
6	13 (33.3 %)	12 (26.7 %)		4 (18.2 %)	3 (20.0 %)	
7	7 (17.9 %)	14 (31.1 %)		12 (54.5 %)	5 (33.3 %)	
8	11 (28.2 %)	14 (31.1 %)		2 (9.1 %)	6 (40.0 %)	
9	7 (17.9 %)	4 (8.9 %)		4 (18.2 %)	1 (6.7 %)	
10	1 (2.6 %)	1 (2.2 %)		0 (0.0 %)	0 (0.0 %)	

fPSA: free prostate-specific antigen; n: numbers of patients; NA: not available; PZ: peripheral zone; TCM: traditional Chinese medicine; TPSA: total prostate-specific antigen; TZ: transition zone; *P: value < 0.05.

3. Results

3.1. Patient demographic data

A total of 121 PCa patients were eligible for this study, including 84 patients in the training cohort and 37 patients in the validation cohort. The detailed TCM syndrome and clinical characteristics of the patients in the training and validation cohorts are listed in Table 1. There were no significant differences in patient's age, TPSA, free PSA, lesion number, location, maximum tumor diameter, MRI T-stage, and Gleason score between PCa with TCM excess syndrome group and PCa with TCM deficiency syndrome group in both training and validation cohorts ($P > 0.05$), except for lesion number in the training cohort.

3.2. Radiomic signature development

The 1316 radiomic features were dimensionally reduced by using the mRMR algorithm and the LASSO algorithm to construct the radiomic models of T2WI, DWI and ADC, separately presented in Supplementary Figs. 1–3. The 14 selected features extracted from the ADC imaging were developed the ADC model (Fig. 2). The 17 selected features extracted from T2WI and DWI were consequently conducted into the T2WI and DWI models, respectively (Fig. 2). The rad-scores of PCa with TCM excess syndrome were higher than those of deficiency syndrome PCa in the training and validation cohorts ($p < 0.05$, Fig. 3).

3.3. Performance and comparison

The radiomic signature of the T2WI, DWI and ADC models demonstrated good performance for the classification of TCM deficiency and excess syndrome in the training and validation cohorts (Fig. 4). The ADC model had the best discrimination in separating patients with TCM excess syndrome and deficiency syndrome, and its accuracy, sensitivity, specificity and AUC were 78.8 %, 70.8 %; 90.7 %, 72.2 %; 66.7 %, 83.3 %; 0.847, 0.809 in the training and validation cohorts, respectively (Table 2). DeLong's comparison displayed there were no significant differences among the model of T2WI, DWI and ADC ($P > 0.05$) both in the training and validation cohorts.

The calibration curve demonstrated that there was good agreement between the prediction based on the ADC, DWI and T2WI model and the actual diagnosis in the training and validation cohorts (Fig. 5). The Hosmer Lemeshow test showed there were no significant differences ($P > 0.05$) in the training and validation cohorts presented in Supplementary Table s3 and Figs. s4–7.

4. Discussion

In this study, we have developed and validated MRI-based radiomic models to differentiate PCa patients with TCM excess syndrome from PCa patients with deficiency syndrome. The radiomic signature of the T2WI, DWI and ADC models demonstrated good performance for the classification of TCM deficiency and excess syndrome in both cohorts. The radiomic approach can be more objective and accurate TCM syndrome differentiation on the basis of traditional clinical symptoms, tongue coating and pulse. Therefore, the results shown herein indicate that MRI radiomics can be used as a potential, non-invasive quantitative tool for TCM deficiency and deficiency syndrome differentiation in PCa.

Currently, there are no standard criteria for TCM syndrome differentiation, which limits its widely clinical application. It is necessary to absorb the advantages and means of modern medicine diagnosis and treatment so as to differentiate TCM syndrome objectively [7]. A study [21] has reported that colorectal cancer patients with different TCM syndromes, such as excess syndrome, deficiency syndrome and deficiency-excess syndrome had significant differences in the distribution of cell subsets using a single cell RNA sequencing analysis. Wang et al. [22] showed that there were significant differences in the laboratory indicators in the colorectal cancer patients with different TCM syndrome. They believed that total bilirubin, hemoglobin, uric acid, and hematocrit may be served as reliable indicators for TCM differentiation of colorectal cancer patients. As far as we know, there was seldom study on the prediction of TCM syndrome types using radiomics approach in PCa. We found that the radiomic signature of the T2WI, DWI and ADC models

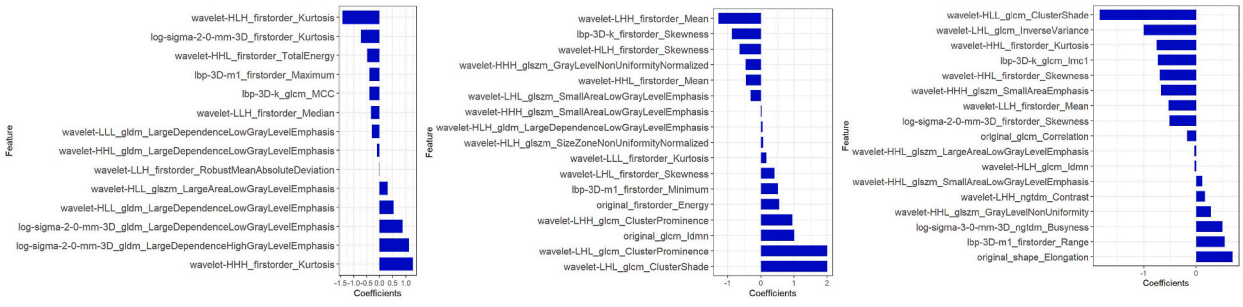

Fig. 2. The selected features to build radiomic models of ADC, DWI and T2WI. Abbreviations: ADC, apparent diffusion coefficient; DWI, diffusion-weighted imaging; T2WI, T2 weighted imaging.

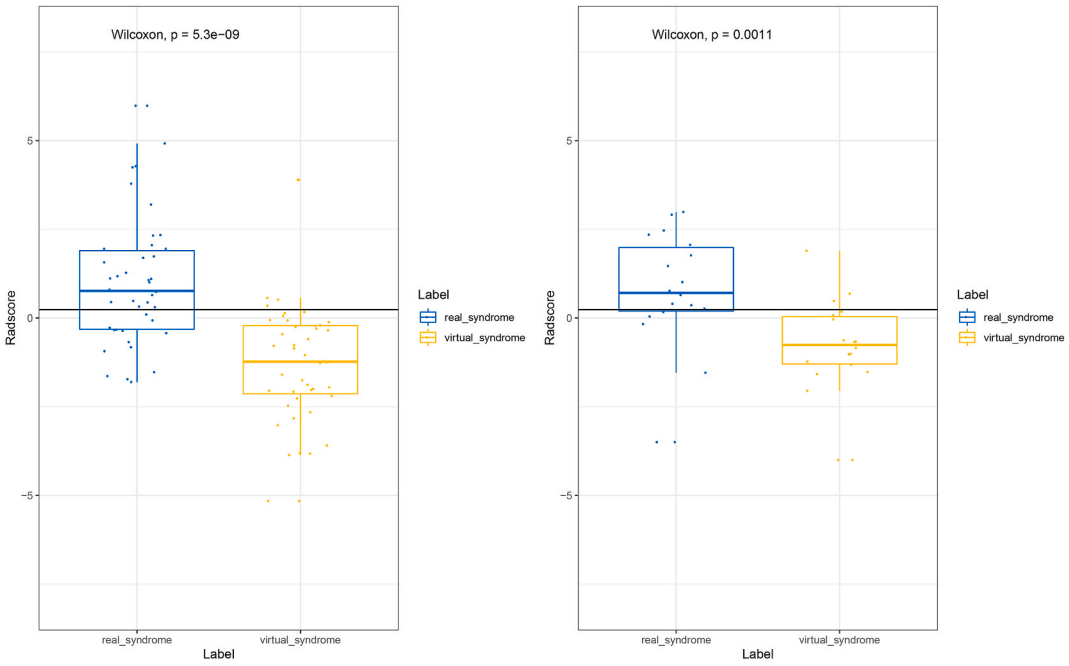

Fig. 3. The boxplots describing the radiomic models of ADC between TCM deficiency syndrome group and excess syndrome group in both the training and validation cohorts, which have significant differences. Abbreviations: Real_syndrome, excess syndrome group; virtual_syndrome, deficiency syndrome group.

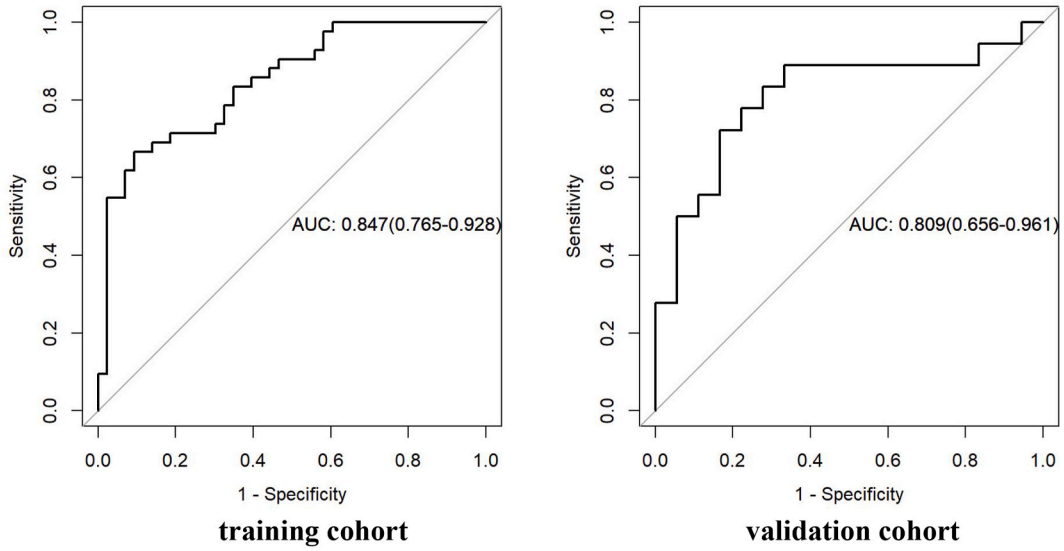

Fig. 4. Receiver operating characteristic (ROC) curve of ADC model for differentiating TCM excess syndrome PCa patients from TCM deficiency syndrome PCa patients in the training and the validation cohorts. Abbreviations: AUC, the area under receiver operating characteristic curve.

have the ability to differentiate PCa with TCM excess syndrome from deficiency syndrome in both cohorts. The radiomic signature directly obtain information from MR imaging and can quantitatively and computationally assess TCM syndromes in PCa patients.

It is worth noteworthy that the radiomic signature of ADC model demonstrates higher discrimination performance than that of the T2WI and DWI models for the classification of TCM deficiency and excess syndrome in PCa. This outcome may be attributed to the fundamental nature of DWI and ADC, which have the capacity to reflect the pathological status of prostate cancer [23]. DWI technology is based on the microscopic movement of water molecules, which can non-invasive evaluate the diffusion degree of water molecules inside human tissues, reflecting the density of tissue cells. DWI have been regarded as the dominant weight sequence for evaluating peripheral zone [9,10]. The ADC value is considered as a reproducible quantitative marker for evaluating the invasiveness

Table 2
Predictive performance of the radiomic model in the training and validation cohorts.

Model	AUC (95 % CI)	Sensitivity	Specificity	Accuracy	PPV	NPV
Training cohort						
T2WI model	0.824 (0.730–0.914)	0.721	0.833	0.776	0.816	0.745
DWI model	0.824 (0.732–0.915)	0.884	0.690	0.788	0.745	0.853
ADC model	0.847 (0.765–0.928)	0.907	0.667	0.788	0.736	0.875
Validation cohort						
T2WI model	0.759 (0.603–0.916)	0.444	0.944	0.694	0.889	0.630
DWI model	0.750 (0.578–0.922)	0.944	0.611	0.778	0.708	0.917
ADC model	0.809 (0.656–0.961)	0.722	0.833	0.778	0.813	0.750

AUC: area under the receiver operating characteristic curve; 95 % CI: 95 % confidence interval; NPV: negative predictive value; PPV: positive predictive value.

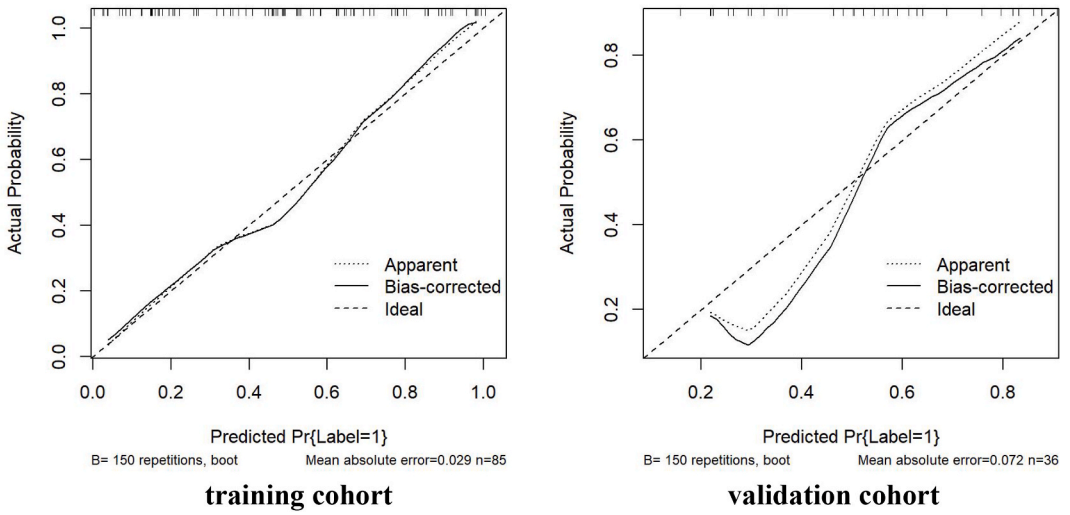

Fig. 5. The calibration curve of ADC model predicting PCa patients with TCM excess syndrome in the training and the validation cohorts. The calibration curve evaluates the consistency between the ADC model prediction and the actual diagnosis of PCa with TCM excess syndrome. Abbreviations: Pr, probability.

in PCa [24]. Furthermore, it is essential to emphasize the interconnection between TCM syndrome and the pathology of prostate cancer. The distribution of TCM syndromes in PCa patients is mainly based on excess symptoms such as qi stagnation and blood stasis in the early stage, and mainly on deficiency symptoms such as spleen and kidney deficiency in the later stage [25].

Note that most of the selected radiomic features constructed in the T2WI, DWI, and ADC models were wavelet features. It is likely explained that there is an underlying relationship between wavelet features and TCM syndromes in PCa. The wavelet transform is a multiscale image analysis method that segments three-dimensional image data into different frequency components along three axes [26]. This observation was consistent with former studies which adopted wavelet-based features in the radiomics models. A radiomics study employed support vector machine to preoperatively evaluate lymph node status in patients with intrahepatic cholangiocarcinoma [27]. The prediction model was built using five radiomic features, all of which were wavelet features. These studies demonstrated that wavelet features were notable imaging biomarkers for predicting the grade and aggressiveness of tumors because they were dramatically associated with the pathological change.

In this study, manual tumor delineation is indeed time-consuming. A single experienced radiologist delineated all lesions to maintain accuracy and consistency across all ROIs. In addition, when sketching on MRI, pathological results were taken as the standard. Currently, there are certain difficulties in an automated tumor segmentation method for prostate cancer. A study conducted by Young et al. demonstrated that the performance of a deep learning-based algorithm (DLA) reached the level of inexperienced radiologists in detecting and PI-RADS classification of focal lesions in prostate MRI [28]. Therefore, manual tumor delineation performed by experienced radiologist have high accuracy and consistency in the study.

This study still has several limitations. Firstly, the study was a retrospective study and the sample size is relatively small. The predictive value of radiomics based MR imaging for TCM syndrome types requires prospective study, which means that the results need to be verified or confirmed by using larger sample sizes with various TCM syndrome patterns of PCa patients. Secondly, patients with lesions less than 5 mm in diameter on MR imaging were excluded because we could not delineate PCa region segmentation in MR imaging. This may lead to patient selection bias. While the study has several limitations, we believe that this study methodology strategy provides adequate validation of the main findings.

5. Conclusions

The radiomic signature based on MR imaging can be performed as a non-invasive approach to provide some objective basis for discrimination TCM deficiency syndrome from excess syndrome in PCa, in which ADC model has the best diagnostic efficiency. Further prospective studies with large size of samples are necessary to confirm our preliminary results. With further research, the radiomic model may be objectively applied to TCM syndromes classification in PCa.

Data availability

All data for evaluating the conclusions are present in this paper. Additional data related to this study can be obtained from the corresponding authors upon reasonable request.

Funding

This work was partly supported by the Chinese Medical Health Science and Technology Project of Zhejiang Provincial Health Commission (2022ZA102), the Medical Health Science and Technology Project of Zhejiang Provincial Health Commission (2022KY996) and Hangzhou Social Development Research Project (202204B07).

CRediT authorship contribution statement

Yongsheng Zhang: Writing – review & editing, Writing – original draft. **Huan Yang:** Writing – review & editing, Writing – original draft. **Zhiping Li:** Writing – original draft, Conceptualization. **Chen Gao:** Data curation, Conceptualization. **Yin Chen:** Formal analysis. **Yasheng Huang:** Investigation, Formal analysis. **Xianjie Yue:** Methodology. **Chang Shu:** Investigation, Formal analysis. **Yuguo Wei:** Software, Formal analysis, Data curation. **Feng Cui:** Writing – review & editing, Visualization, Project administration, Formal analysis, Conceptualization. **Maosheng Xu:** Writing – review & editing, Supervision, Project administration, Conceptualization.

Declaration of competing interest

The authors declare the following financial interests/personal relationships which may be considered as potential competing interests:Yongsheng Zhang reports article publishing charges was provided by the Chinese Medical Health Science and Technology Project of Zhejiang Provincial Health Commission. Zhiping Li reports article publishing charges was provided by the Medical Health Science and Technology Project of Zhejiang Provincial Health Commission. Feng Cui reports article publishing charges was provided by Hangzhou Social Development Research Project. Yuguo Wei reports a relationship with Global Medical Service, GE Healthcare that includes: employment. If there are other authors, they declare that they have no known competing financial interests or personal relationships that could have appeared to influence the work reported in this paper.

Acknowledgements

Not applicable.

Appendix A. Supplementary data

Supplementary data to this article can be found online at https://doi.org/10.1016/j.heliyon.2023.e23242.

References

[1] F. Bray, J. Ferlay, I. Soerjomataram, R.L. Siegel, L.A. Torre, A. Jemal, Global cancer statistics 2018: GLOBOCAN estimates of incidence and mortality worldwide for 36 cancers in 185 countries, Cancer J Clin 68 (6) (2018) 394–424.
[2] Z.T. Fu, X.L. Guo, S.W. Zhang, R.S. Zheng, H.M. Zeng, Chen Ru. Statistical analysis of incidence and mortality of prostate cancer in China, 2015, Chin. J. Oncol. 42 (9) (2020) 718–722.
[3] A. Lu, M. Jiang, C. Zhang, K. Chan, An integrative approach of linking traditional Chinese medicine pattern classification and biomedicine diagnosis, J. Ethnopharmacol. 141 (2) (2012) 549–556.
[4] X.Q. Liu, R.S. Zhang, X.Z. Zhou, H. Zhou, Y.Y. He, S. Han, et al., Analysis of Chinese medical syndrome features of ischemic stroke based on similarity of symptoms subgroup, Chin. J. Integr. Med. (2022), 35723812.
[5] F.C. Si, C.F. Du, Analysis of TCM syndromes and prescriptions rules in prostatic carcinoma, Chinese Journal of Traditional Chinese Medicine (Chin) 30 (2) (2015) 581–585.
[6] Y.J. Jia, J. Chen, X.J. Li, X.Q. Wang, W.T. Xu, Literature analysis on TCM syndrome of prostate cancer, Liaoning Journal of Traditional Chinese Medicine (Chin) 41 (9) (2014) 1850–1852.
[7] N. Li, J. Yu, X. Mao, Y. Zhao, L. Huang, The research and development thinking on the status of artificial intelligence in traditional Chinese medicine, Evid Based Complement Alternat Med 2022 (2022), 7644524.

[8] J.E. Thompson, P.J. van Leeuwen, D. Moses, R. Shnier, P. Brenner, W. Delprado, et al., The diagnostic performance of multiparametric magnetic resonance imaging to detect significant prostate cancer, J. Urol. 195 (5) (2016) 1428–1435.
[9] J.C. Weinreb, J.O. Barentsz, P.L. Choyke, F. Cornud, M.A. Haider, K.J. Macura, et al., PI-RADS prostate imaging - reporting and data system: 2015, version 2, Eur. Urol. 69 (1) (2016) 16–40.
[10] B. Turkbey, A.B. Rosenkrantz, M.A. Haider, A.R. Padhani, G. Villeirs, K.J. Macura, et al., Prostate imaging reporting and data system version 2.1: 2019 update of prostate imaging reporting and data system version 2, Eur. Urol. 76 (3) (2019) 340–351.
[11] S.S. Yip, H.J. Aerts, Applications and limitations of radiomics, Phys. Med. Biol. 61 (13) (2016) R150–R166.
[12] X. Min, M. Li, D. Dong, Z. Feng, P. Zhang, Z. Ke, et al., Multi-parametric MRIbased radiomics signature for discriminating between clinically significant and insignificant prostate cancer: cross-validation of a machine learning method, Eur. J. Radiol. 115 (2019) 16–21.
[13] Y. Zhang, W. Chen, X. Yue, J. Shen, C. Gao, P. Pang, et al., Development of a novel, multi-parametric, MRI-based Radiomic nomogram for differentiating between clinically significant and insignificant prostate cancer, Front. Oncol. 10 (2020) 888.
[14] F. Cheung, TCM: made in China, Nature 480 (7378) (2011) S82–S83.
[15] Daihan Zhou, Oncology of Traditional Chinese Medicine, first ed., China Press of Traditional Chinese Medicine (Chin), Beijing, 2011, pp. 308–315.
[16] G.J.L.H. van Leenders, T.H. van der Kwast, D.J. Grignon, A.J. Evans, G. Kristiansen, C.F. Kweldam, et al., The 2019 international society of urological pathology (ISUP) consensus conference on grading of prostatic carcinoma, Am. J. Surg. Pathol. 44 (8) (2020) e87–e99.
[17] E. Baco, O. Ukimura, E. Rud, L. Vlatkovic, A. Svindland, M. Aron, et al., Magnetic resonance imaging–transectal ultrasound image-fusion biopsies accurately characterize the index tumor: correlation with step-sectioned radical prostatectomy specimens in 135 patients, Eur. Urol. 67 (4) (2015) 787–794.
[18] J.D. Le, N. Tan, E. Shkolyar, D.Y. Lu, L. Kwan, L.S. Marks, et al., Multifocality and prostate cancer detection by multiparametric magnetic resonance imaging: correlation with whole-mount histopathology, Eur. Urol. 67 (3) (2015) 569–576.
[19] P.H. Carroll, J.L. Mohler, NCCN Guidelines updates: prostate cancer and prostate cancer early detection, J Natl Compr Canc Netw 16 (5S) (2018) 620–623.
[20] P. Paul, M.L. Pennell, S. Lemeshow, Standardizing the power of the Hosmer-Lemeshow goodness of fit test in large data sets, Stat. Med. 32 (1) (2013) 67–80.
[21] Y. Lu, C. Zhou, M. Zhu, Z. Fu, Y. Shi, M. Li, et al., Traditional Chinese medicine syndromes classification associates with tumor cell and microenvironment heterogeneity in colorectal cancer: a single cell RNA sequencing analysis, Chin. Med. 16 (1) (2021) 133.
[22] Y.N. Wang, M. Zou, D. Wang, Z.K. Zhang, L.P. Qu, J. Xu, et al., An exploratory study on TCM syndrome differentiation in preoperative patients with colorectal cancer assisted by laboratory indicators, 14, Heliyon 8 (8) (2022), e10207.
[23] A. Chatterjee, G. Watson, E. Myint, P. Sved, M. McEntee, R. Bourne, Changes in epithelium, stroma, and lumen space correlate more strongly with gleason pattern and are stronger predictors of prostate ADC changes than cellularity metrics, Radiology 277 (2015) 751–762.
[24] A. Hoang Dinh, C. Melodelima, R. Souchon, J. Lehaire, F. Bratan, F. MègeLechevallier, et al., Quantitative analysis of prostate multiparametric MR images for detection of aggressive prostate cancer in the peripheral zone: a multiple imager study, Radiology 280 (2016) 117–127.
[25] Z.Q. Chen, S.S. Wang, Z.G. Bai, Z.H. Wang, L.G. Lv, C.M. Gu, et al., Staging based strategies and practice for prostate cancer, Chinese Journal of Integrated Traditional and Western Medicine (Chin) 36 (6) (2016) 749–752.
[26] A. Kassner, R. Thornhill, Texture analysis: a review of neurologic MR imaging applications, AJNR Am J Neuroradiol 31 (5) (2010) 809–816.
[27] L. Xu, P. Yang, W. Liang, W. Liu, W. Wang, C. Luo, et al., A radiomics approach based on support vector machine using MR images for preoperative lymph node status evaluation in intrahepatic cholangiocarcinoma, Theranostics 9 (18) (2019) 5374–5385.
[28] S.Y. Youn, M.H. Choi, D.H. Kim, Y.J. Lee, H. Huisman, E. Johnson, et al., Detection and PI-RADS classification of focal lesions in prostate MRI: performance comparison between a deep learning-based algorithm (DLA) and radiologists with various levels of experience, Eur. J. Radiol. 142 (2021), 109894.